Advanced Composite Materials
Publication details, including instructions for authors and subscription information:
http://www.tandfonline.com/loi/tacm20

High temperature crack sealant based on SiO2-B2O3 for SiC coating on carbon-carbon composites

Hiroshi Hatta , Takayuki Sohtome , Yutaka Sawada & Azusa Shida

Version of record first published: 02 Apr 2012.

To cite this article: Hiroshi Hatta , Takayuki Sohtome , Yutaka Sawada & Azusa Shida (2003): High temperature crack sealant based on SiO2-B2O3 for SiC coating on carbon-carbon composites , Advanced Composite Materials, 12:2-3, 93-106

To link to this article: http://dx.doi.org/10.1163/156855103772658498

Adv. Composite Mater., Vol. 12, No. 2-3, pp. 93–106 (2003)

High temperature crack sealant based on SiO_2-B_2O_3 for SiC coating on carbon–carbon composites

HIROSHI HATTA [1,*], TAKAYUKI SOHTOME [2], YUTAKA SAWADA [2]
and AZUSA SHIDA [3]

[1] *Research Division of Space Propulsion, Institute of Space and Astronautical Science, 3-1-1, Yoshinodai, Sagamihara, Kanagawa 229-8510, Japan*
[2] *Tokyo Institute of Polytechnique, 1583 Iiyama, Atsugi, Kanagawa 243-0297, Japan*
[3] *Yokohama City Center for Industrial Technology and Design, 1-1-1 Fukuura, Kanazawa-ku, Yokohama 236-0004, Japan*

Received 25 June 2002; accepted 2 May 2003

Abstract—Crack sealant required for an anti-oxidation SiC-coating on C/C composites was investigated with the intention of finding material effective up to approximately 1800 K. As a sealant, B_2O_3 is known to be effective. However, B_2O_3 rapidly evaporates at temperatures exceeding 1000 K. Hence, mixtures of SiO_2/B_2O_3 at various ratios were examined in regard to their high temperature durability. As a result of oxidation tests, pure B_2O_3 over-coated on a SiC-coated C/C composite was eventually confirmed to exhibit sufficient sealing capability up to 1800 K. This result was shown to be derived by the chemical reaction between B_2O_3 and SiC. By this reaction, a sufficient amount of SiO_2 was thickly and uniformly formed on the surface of the SiC coating.

1. INTRODUCTION

Carbon fiber reinforced carbon matrix composites (C/Cs) are easily oxidized at temperatures exceeding 700 K [1, 2]. To prevent oxidation, C/Cs are generally used with an anti-oxidation coating [3–6]. However, since the thermal expansion of the C/Cs is extremely low [7], the coating usually experiences severe cracking due to a huge thermal expansion mismatch between the substrate C/C and the coating when the material cools from the coating treatment temperature [3–5]. Thus, a glass sealant is frequently applied to block the oxygen ingress through these cracks.

In the present study, a crack sealant with high temperature capability exceeding 1800 K was explored. The properties required for the crack sealant are [8, 9]:

---

[*] To whom correspondence should be addressed. E-mail: hatta@pub.isas.ac.jp

(1) low oxygen permeability;

(2) superior wettability for easy penetration into cracks;

(3) low melting point so as to comply with the changes of crack openings with temperature;

(4) easy sealing treatment.

Based on these requirements, B_2O_3 has been used [8, 9] as a crack sealant. However, B_2O_3 rapidly evaporates at temperatures exceeding 1100 K, and thus a sealant possessing higher temperature capability is strongly required. In the present study, a sealant based on two constituents, SiO_2-B_2O_3, was examined for the increase of high temperature durability up to about 1800 K. Thus, the sealing performances of various ratios of SiO_2-B_2O_3 over-coated on SiC-coated C/Cs were evaluated using thermogravimetric analysis.

2. EXPERIMENTAL

2.1. Materials

2.1.1. SiC-coated C/C composite. The C/C composite used as a substrate was fabricated using the preformed yarn method [10] and supplied by Across corporation of Japan. This C/C was reinforced with a 50% volume fraction of Torayca M40 (Toray Co., Japan) in cross-ply lamination, and heat-treated at 2273 K. The C/C was supplied with dimensions of 300 × 300 × 3 mm, and cut into 4 × 4 × 3 mm pieces for SiC coating treatment.

The C/C squares were polished with diamond paste. During polishing, the diameter of the diamond paste was gradually reduced from 15 μm to 1 μm. SiC was coated onto the polished surfaces by the chemical vapor deposition (CVD) process after conversion treatment [11, 12]. The conversion treatment was performed in order to reinforce the coating interface by means of a chemical reaction between the gas phase $SiCl_4$ and the carbon of the substrate C/C. Details of the coating treatment have been described elsewhere [11]. In the present paper, the conversion and coating treatments were conducted at 1473 or 2073 K. The thickness of the conversion layer was set to several microns, and the thicknesses of the CVD layers were 40 and 150 μm.

2.1.2. Sealing treatment. The sol-gel method was used to prepare various mixing ratios of SiO_2/B_2O_3 as a glass sealant. The advantage of this process is the production of sealant at a low temperature. The cracks in SiC coating widely open at low temperature but close at the coating treatment temperature. The sealing treatment was performed as follows:

(1) preparation of sol from the hydrolysis of metal alkoxide, a mixture of tetraethoxysilane, $Si(C_2H_5O)_4$, and trimethoxybolane, $B(CH_3O)_3$, (Wako-Jyunyaku, Japan);

(2) dip-coating the sol onto a SiC-coated C/C in a vacuum in order to infiltrate the sol into cracks in the SiC coating;

(3) heat-treatment at 873 K in a furnace in an argon atmosphere.

The molar ratios of SiO_2 to B_2O_3 were set to 10 : 0, 7 : 3, 5 : 5, 3 : 7, and 0 : 10.

2.1.3. SiO_2-B_2O_3 powder and SiC plate. In addition to investigating the sealing-treated SiC-coated C/C, the oxidation and evaporation behaviors of SiO_2-B_2O_3 powder and a SiC plate were examined. For this purpose, SiO_2 and B_2O_3 reagents supplied by Wako-Junyaku of Japan were mixed. To observe oxidation behavior of monolithic SiC, pure SiC disks with diameters of 5 mm and thicknesses of 0.65 mm, were cut from a SiC wafer made using the same thermal CVD process by Toshiba Ceramic Corp.

2.2. Oxidation tests

Oxidation tests were carried out using a thermogravimetry analyzer, Ulvac TGD-9600, for bare, SiC-coated, and glass sealed C/C composites, and a glass over-coated SiC plate to confirm the effects of sealing. These oxidation tests were performed under a dry air flow of 200 ml/min at constant temperatures between 873 and 1873 K for 1000 min. In the rising temperature phase during these tests, argon gas was introduced at a flow rate of 200 ml/min in order to prevent the specimens from oxidation. The thermo-gravimetry analyzer was also used to determine the evaporation rates of the sealant materials, i.e. powder mixtures of various ratios of SiO_2 and B_2O_3. In order to confirm interaction between SiC coating and glass sealant, oxidation tests were also performed on the SiC disk.

2.3. Micro-observations

In order to examine interfacial bonding between the sealant and the SiC coating, cross-sections and surfaces of the sealants were observed before and after oxidation tests using an optical microscope, a scanning electron microscope (SEM), and an electron-probe micro-analyzer (EPMA). The EPMA was used to observe the variation of constituents in the sealant layer during the oxidation tests. Using an optical microscope equipped with a furnace capable of a maximum temperature of 1823 K, variations of the coating-crack opening with temperature as well as evaporation and melting temperatures of the sealants were determined. In these experiments, evaporation points were determined based on the initiation of bubble formation.

3. RESULTS AND DISCUSSION

3.1. SiC-coated C/C composite

3.1.1. Cracks in the SiC coating. For later convenience, the distribution of the crack-opening width in the SiC coating formed at 2073 K was determined from

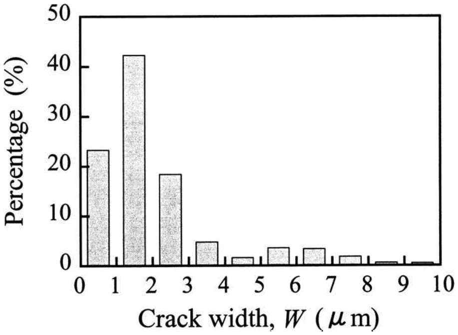

Figure 1. Distribution of the crack widths in SiC coating deposited on a C/C composite.

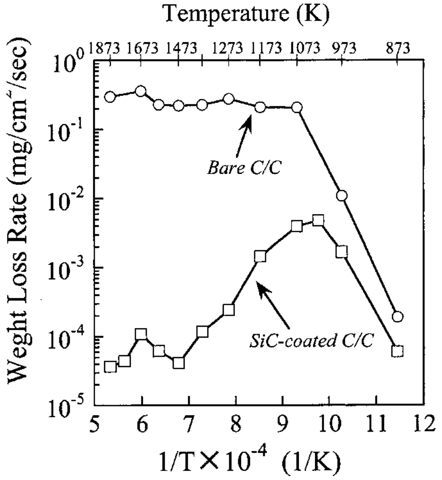

Figure 2. Arrhenius plots of oxidation rates for bare and SiC-coated C/C composites.

optical microscope images. As shown in Fig. 1, the maximum width was about 10 μm and the average was 2–3 μm. The width of the coating cracks linearly decreased with temperature and vanished at the coating treatment temperature [4, 5].

3.1.2. Oxidation rate of SiC coated C/C composite. To provide base line data, the oxidation rates of bare and SiC-coated C/C composites were determined based on the initial gradient of weight loss curves [4]. As shown in Fig. 2, an oxidation rate of the SiC-coated C/C increases up to 1100 K and decreases from 1100 K with temperature. As has been reported previously [4, 5], the oxidation rate is governed by the rate of the chemical reaction between oxygen and carbon below 1100 K, and by oxygen diffusion through the coating cracks above 1100 K. The decrease of the oxidation rate of the SiC-coated C/C composite above 1100 K was caused by the closing of the coating cracks with temperature increase.

Table 1.
Values of parabolic kinetics constant/B for SiC

Temperature (K)	B ($nm^2\ min^{-1}$)
1173	5
1273	49
1373	188
1473	404
1573	777
1673	1406
1773	3365
1873	7056

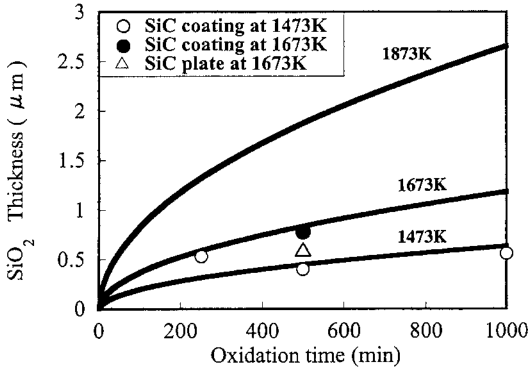

Figure 3. Silica glass thicknesses on a SiC plate and SiC coating during oxidation tests under constant temperatures.

3.1.3. Sealing effect by SiO_2 formation. At elevated temperatures, SiC is oxidized to form SiO_2. In this reaction, the volume of the resultant SiO_2 becomes about twice as large as that of the original SiC. Thus, the formed SiO_2 narrows the opening of the coating cracks. The forming rate of SiO_2 from SiC has been given by Filipuzzi *et al.* [13]. Time dependence of the formed SiO_2 thickness x obeys the parabolic law given by equation (1) with the rate constant B given in Table 1,

$$x = B^{1/2} \times t^{1/2}, \tag{1}$$

where t denotes oxidation time (min). The calculated value of x is compared with the experimental results in Fig. 3, where the solid lines represent calculation results, and the symbols show the experimental results using the CVD-SiC formed by ourselves and that using the purchased SiC wafer. It can be seen in this figure that the calculated SiO_2 thickness agreed reasonably with the experimental observations, and that the thickness within our experimental conditions was under 1 μm. Since the maximum crack width was larger than 10 μm in room temperature, it cannot be expected that the volumetric expansion due to the SiC oxidation completely closes the coating cracks.

3.2. SiO_2-B_2O_3 sealant

3.2.1. Bonding of SiO_2-B_2O_3 with SiC coating. Optical micro-photographs of the surfaces of SiO_2-B_2O_3 over-coatings with a thickness of about 30 μm on the SiC-coated C/C composite are shown in Fig. 4a–d, where (a) represents the photograph for SiC coating without sealant, (b) pure B_2O_3, (c) $SiO_2 : B_2O_3$, 1 : 1, and (d) pure SiO_2. As shown in these figures, while a uniform and well-bonded over-coating was formed for the pure B_2O_3, intensive cracks in the over-coating and debonding along the interface between the over-coating and the SiC-coating were observed for the pure SiO_2. In the intermediate case of $SiO_2 : B_2O_3$, 1 : 1, cracks but no debonding were seen. These results indicate that mixing of SiO_2 into B_2O_3 deteriorates the wettability with SiC coating. However, even for simple SiO_2, the over-coating could be formed without debonding when the thickness was thinner than 5 μm.

Figure 5 shows the cross-sections around the cracks in the SiC coating for the over-coatings of pure B_2O_3 (a) and pure SiO_2 (b). These figures clearly show that B_2O_3-SiO_2 easily infiltrates into cracks in the SiC coating and seals the C/C substrates.

3.2.2. Melting and evaporation of SiO_2-B_2O_3. Since the crack width in the SiC coating varies with temperature, the sealing material should be liquid so as to adjust its shape in service temperatures. In addition, the sealant is required not to evaporate rapidly. The melting points (T_ms) and evaporation temperatures (T_es) of the SiO_2-B_2O_3 mixtures were determined by direct observation using an optical microscope with a furnace as a function of their mixing ratio (r_m). These experiments were performed on SiC-coated C/C. Figure 6 shows the experimental results, where the open squares represent T_ms and the filled squares T_es, at which bubbles began to appear. As this figure shows, T_m and T_e increased with increasing fractions of SiO_2, and T_m agrees with the reference data [14]. However, the entire region between T_m and T_e is not effective for sealing. Pure B_2O_3 effectively wetted the SiC coating and spread to form a uniform film over it, but when the SiO_2 fraction surpassed 50%, the wettability deteriorated to produce ball-like condensation of the mixture, as shown in Fig. 7. The condensed sealant cannot cover substrate and thus might not be admitted as the sealant. By adoption of the criterion of non-condensation, the effective range for the sealant was determined as shown by a shaded area in Fig. 6. Thus, the maximum temperature for the sealant was improved about 200 K by the mixing of SiO_2 with B_2O_3.

Figure 8 shows evaporation rates for various ratios of SiO_2-B_2O_3 as a function of temperature. It follows from this figure that the evaporation rate is lowered by the addition of SiO_2. However, within the above described effective range, the improvement is not noticeable.

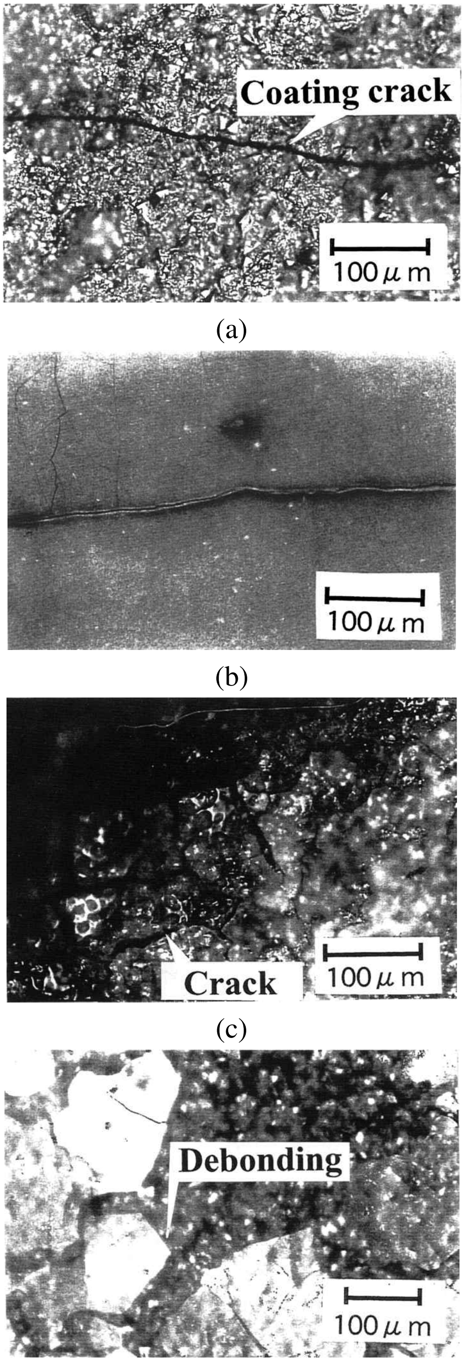

(a)

(b)

(c)

(d)

Figure 4. Optical micro-photographs for surfaces of SiC coating and over-coatings observed at room temperature. (a) SiC coating (without sealing); (b) over-coatings of pure B_2O_3 (100%); (c) SiO_2/B_2O_3 (50%/50%), and (d) pure SiO_2 (100%).

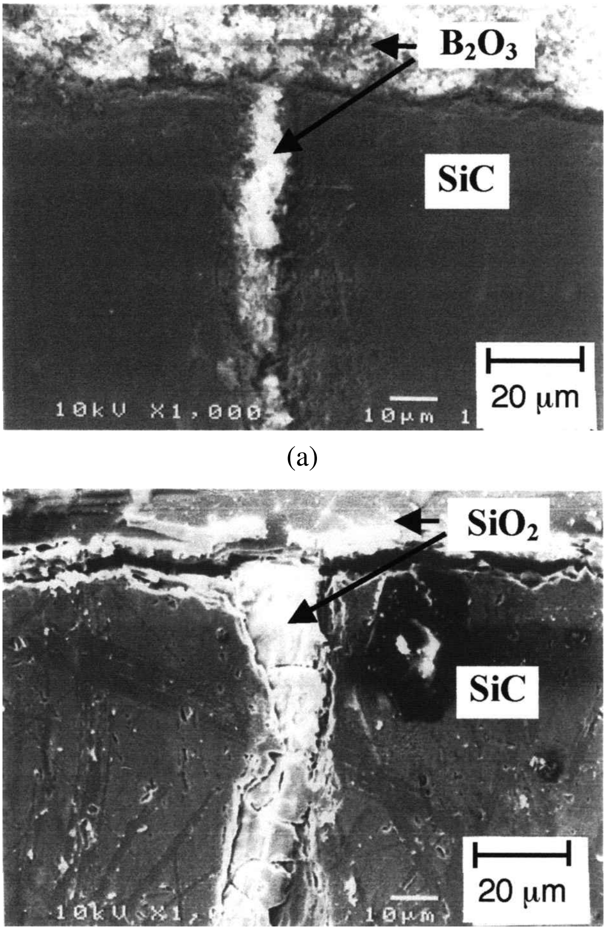

(a)

(b)

Figure 5. Scanning electric micro-photographs of cross-sections of SiC coatings with sealants of pure B_2O_3 (100%) (a) and pure SiO_2 (100%) (b).

3.3. Interaction between sealant and SiC

3.3.1. Oxidation behavior of sealed C/C. At elevated temperatures, weight change of SiC-coated C/Cs with sealing treatment was expected to occur in the steps shown in Fig. 9, i.e.

(1) evaporation of the sealant covering the entire surface;

(2) evaporation of the sealant filled in coating cracks;

(3) oxidation of substrate C/C.

In order to confirm these steps, the time interval required for complete evaporation of glass sealant was calculated on the basis of the data shown in Fig. 8, 5.68×10^{-7} g/s/cm^2 at 1473 K, where evaporation was assumed to occur in proportion to the surface area of B_2O_3. The calculated results were then compared with

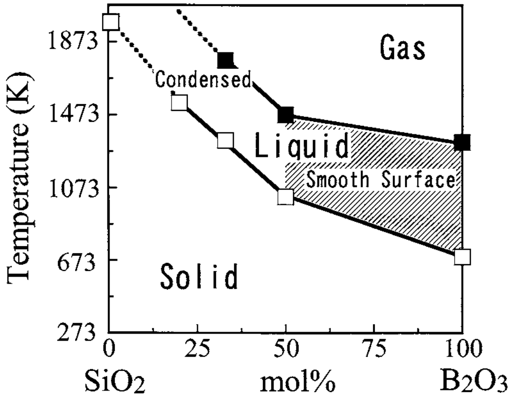

Figure 6. Phase diagram of SiO_2/B_2O_3 glass determined from observations using a high temperature microscope.

Table 2.
Thickness of B_2O_3 glass-sealant treated SiC-water in the heat treatment tests

		500 min	1000 min
1473 K	Air		12 μm
	Argon		6 μm
1673 K	Air	27 μm	
	Argon	14 μm	
1873 K	Air	29 μm	

experimental results as shown in Fig. 10. In the calculation, the following data for a SiC-coated cross-ply laminated C/C of about 4 × 4 × 3 mm, coating thickness 40 μm, were used: weight of B_2O_3, 3.68 mg; surface area of SiC coating, 0.773 cm^2; crack opening area of the SiC coating, 0.0025 cm^2. The crack opening area was determined using the data shown in Fig. 1 and average value of crack spacing (distance between adjacent cracks) [4]. This calculation result is shown by the dashed line in Fig. 10 with the above-mentioned processes, (1), (2), and (3), corresponding to the numbers in the figure. As this figure shows, contrary to the prediction, process (3) did not appear even after a sufficiently longer time has passed. Observation of the specimen after high temperature exposure revealed that a glass-like material thinly covered the specimen surface and filled cracks in the coating. This result obviously indicates that some phenomenon other than that in the above model occurred.

In order to understand this anomalous behavior, B_2O_3 was coated on a SiC plate without C/C, and high-temperature exposure experiments were performed in air and argon atmospheres. Figure 11a and b shows the experimental results in air and argon, respectively, and the final thicknesses of the glass-like films are summarized in Table 2. This film was analyzed using EPMA, and constituent atoms in the film were identified to be Si and O. Consequently, the resultant film was confirmed to

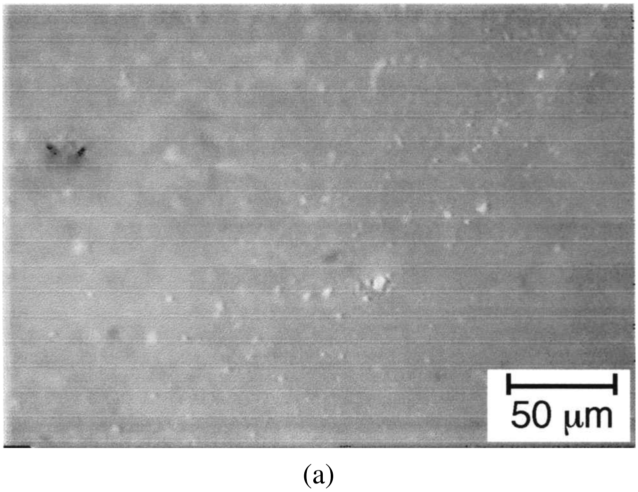

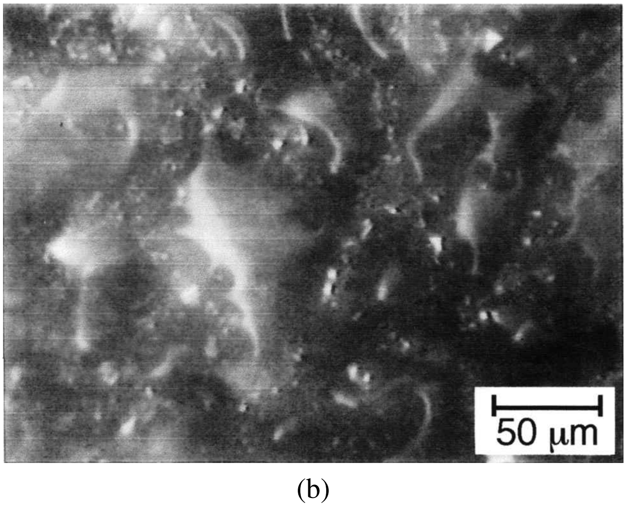

Figure 7. An optical micro-photograph of surfaces of over-coatings observed at elevated temperatures: (a) pure B_2O_3 (100%) (1173 K); (b) SiO_2/B_2O_3 (50%/50%) (1173 K).

be SiO_2. As Fig. 3 indicates, simple oxidation reaction should yield film with a thickness of less than 1 μm. On the SiC plate, however, a far thicker film was formed. Accordingly, it was concluded that the thick SiO_2 film was formed by some interaction between B_2O_3 and SiC.

Two phenomena could be supposed to be involved in the mechanisms yielding such a thick SiO_2 layer. On the interface, SiC reacted with B_2O_3 to form SiO_2. This reaction occurred in the B_2O_3 melting environment. Thus, the resultant SiO_2 easily diffused into B_2O_3 to increase the oxidation reaction rate. In addition to this mechanism, an increase in the diffusion rate of oxygen through B_2O_3 might occur due to the interaction of B_2O_3 and SiO_2 in the air environment. According to Schlichting [9] and Fergus *et al.* [15], when $SiO_2$is mixed into B_2O_3,the oxygen

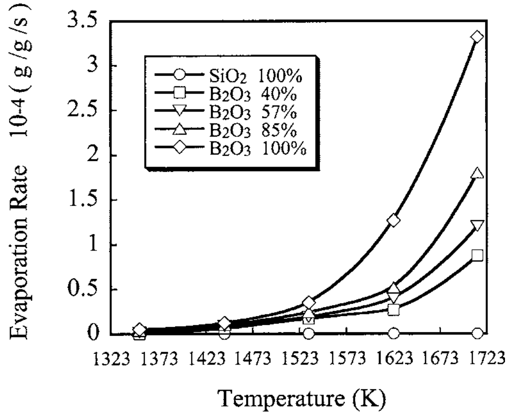

Figure 8. Evaporation rates of glasses with various SiO_2/B_2O_3 ratios.

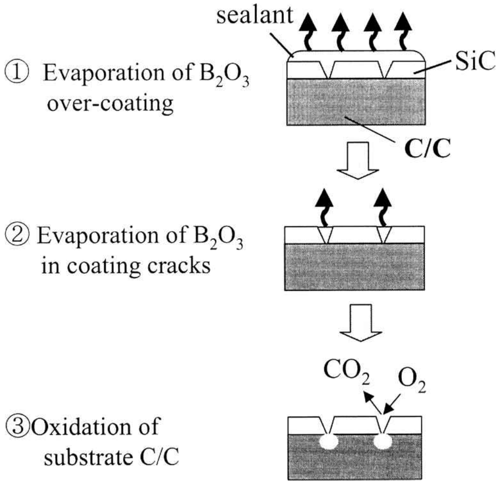

Figure 9. Predicted oxidation behavior of a SiC-coated C/C composite over-coated with volatile glass.

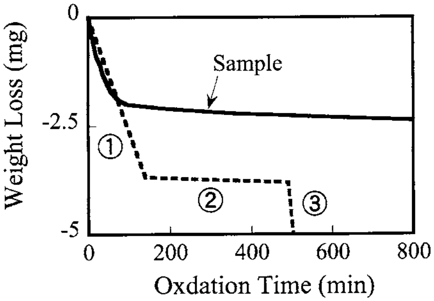

Figure 10. Weight loss of a SiC-coated C/C composite over-coated with B_2O_3 glass. The solid line represents experimental results of an oxidation test performed at 1447 K for 1000 min. The dashed line is the predicted weight loss based on the model illustrated in Fig. 9.

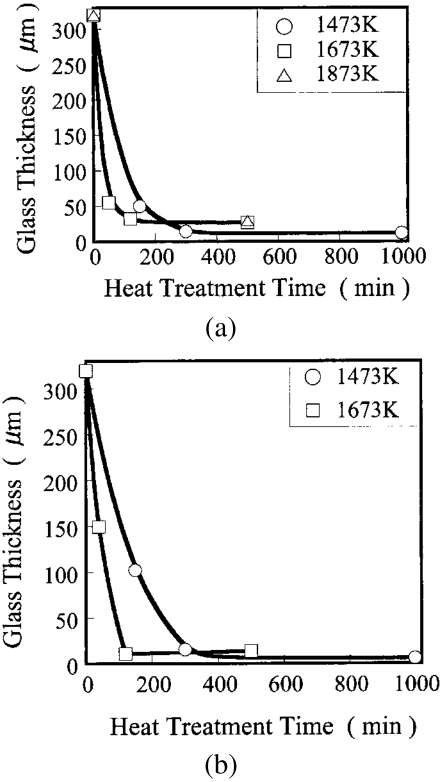

Figure 11. Thickness of glass coating on a SiC plate formed by the interaction of the B_2O_3 coating and the substrate under high temperature environments of dry air (a) and argon (b).

diffusion rate in the mixture is enhanced by loosening the loop structure of B_2O_3. In the present experiments, the discrepancy between air and argon environments was introduced by this mechanism.

The above results clearly show that B_2O_3 on SiC possesses sufficient capability to seal the coating cracks up to 1800 K in the present experimental conditions. A similar phenomenon can be expected when a small amount of SiO_2 is mixed into B_2O_3.

3.3.2. Reaction on the B_2O_3/SiC interface. Let us confirm the above-mentioned chemical reaction. For example at 1473 K, equation (2) is a chemical reaction that possibly produces SiO_2 in an argon atmosphere,

$$7\mathrm{SiC(s)} + 6\mathrm{B_2O_3(l)} \rightarrow 7\mathrm{SiO_2(s)} + 3\mathrm{B_4C(s)} + 4\mathrm{CO(g)} \uparrow \tag{2}$$

The change of free energy (ΔG) by this reaction is given by

$$\begin{aligned} \Delta G = {} & 7\Delta G(\mathrm{SiO_2}) + 3\Delta G(\mathrm{B_4C}) + 4\Delta G(\mathrm{CO}) \\ & - 7\Delta G(\mathrm{SiC}) - 6\Delta G(\mathrm{B_2O_3}) + RT\ln(P_{\mathrm{CO}})^4 \end{aligned} \tag{3}$$

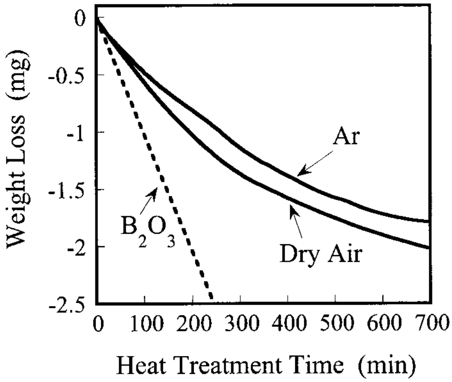

Figure 12. Comparison of evaporation rates of B_2O_3 coating on a SiC plate at 1473 K under environments of dry air and argon.

where R is the gas constant and P_{CO} is the partial pressure of CO. Substitution of free energies at 1473 K [16] yields negative resultant free energy, provided that P_{CO} is less than 0.0381 atm. In an argon environment, this condition should be satisfied. Thus, the reaction is concluded to proceed.

Figure 12 compares weight change of the B_2O_3-coated SiC plate at 1473 K in oxidizing atmosphere with that in argon. All the test results in this figure were reduced to oxidation weight change for the surface area of the TGA-cell (∅ 5 mm). Possible sources of the weight change in an oxidizing environment are given by

$$SiC + 2O_2 \rightarrow SiO_2 + CO_2 \uparrow \tag{4a}$$

$$B_2O_3 \rightarrow B_2O_3 \uparrow \tag{4b}$$

Equation (4a) gives the weight increase but equation (4b) gives the weight decrease. The sum of both the changes yields the solid line in Fig. 12. In contrast, in an argon atmosphere, the reaction of equation (4a) does not occur but equation (2) should be considered. Thus the result in Fig. 12, in which the weight reduction is larger in air than in argon, can be understood due to the production of B_4C in equation (2).

4. CONCLUSION

Various mixtures of SiO_2 and B_2O_3 were investigated as candidates for a high-temperature sealing material on SiC-coated C/C composite. The conclusions obtained are as follows.

(1) When SiO_2 is mixed with B_2O_3, the melting and evaporation temperatures become high and the evaporation rate decreases. The increases of these temperatures were about 200 K.

(2) A new phenomenon was found to improve the high temperature sealing effect of B_2O_3. This phenomenon was based on the chemical interaction between B_2O_3

and SiC and remarkably facilitated SiO_2 formation. This mechanism allows the use of pure B_2O_3 as an effective sealing material over temperatures of 1800 K.

Acknowledgement

This research was partly supported by a grant-in-aid for basic science (grant No. 11305047) from The Ministry of Education, Sports, Culture, Science and Technology of Japan.

REFERENCES

1. E. Yasuda, S. Kimura and Y. Shibusa, *Trans. JSCM* **6**, 14 (1980).
2. D. W. Mckee, *Carbon* **17**, 551–557 (1987).
3. J. R. Strife and J. E. Sheehan, *Ceramic Bulletin* **67**, 369 (1988).
4. T. Aoki, H. Hatta, Y. Kogo and H. Fukuda, *J. Japan Inst. Metals* **62** (4), 404–412 (1998) (in Japanese).
5. H. Hatta, T. Aoki, Y. Kogo and T. Yarii, *Composites: Part A* **30**, 515–520 (1999).
6. S. Uemura, Y. Sohda and Y. Kude, in: *Proc. First Int. Symp. FGM*, p. 273. Elsevier, Amsterdam, The Netherlands (1990).
7. H. Hatta, Y. Kogo, Y. Yoshihara, Y. Sawada, K. Takahashi, K. Hosono and T. Dozono, *Material Systems* **17**, 15–24 (1995) (in Japanese).
8. F. J. Buchanan and J. A. Little, *J. Mater. Sci.* **28**, 2324–2330 (1993).
9. J. Schlichting, *J. Non-Crystalline Solids* **63**, 173–181 (1984).
10. A. Okura and T. Chou, in: *Advanced Composites in Emerging Technologies*, pp. 348–353 (1992).
11. H. Hatta, Y. Nakayama, K. Goto, T. Aoki, Y. Kogo and H. Fukuda, *Trans. JSME* **A65** (638), 2073–2079 (1999) (in Japanese).
12. K. Fujii, H. Imai, S. Nomura and M. Shindo, *J. Nucl. Mater.* **187**, 204–208 (1992).
13. L. Filipuzzi, R. Naslain and C. Jaussaud, *J. Mater. Sci.* **27**, 697 (1992).
14. R. S. Roth, in: *Phase Equilibria Diagrams*, Vol. 11, p. 112. American Ceramic Society (1995).
15. J. W. Fergus and W. L. Worrell, *J. Am. Ceram. Soc.* **78** (7), 1961–1964 (1995).
16. Barin, Ihsan, *Thermochemical Data of Pure Substances* (1995).